International Journal of Nanomedicine

Dovepress
Taylor & Francis Group

Open Access Full Text Article

ORIGINAL RESEARCH

Bone Marrow-Derived Macrophages Loaded with Boron Carbide Nanoparticles Targeting the Glioblastoma Microenvironment for Boron Neutron Capture Therapy

Anna Rudawska[1], Agnieszka Szczygieł[1], Katarzyna Węgierek-Ciura[1], Jagoda Mierzejewska[1], Dawid Kozień[2], Paulina Żeliszewska[3], Monika Chaszczewska-Markowska[1], Piotr Rusiniak[4], Katarzyna Wątor[4], Zbigniew Pędzich[2], Elżbieta Pajtasz-Piasecka[1], Bożena Szermer-Olearnik[1]

[1]Hirszfeld Institute of Immunology and Experimental Therapy, Polish Academy of Sciences, Wrocław, Poland; [2]Department of Materials Science and Ceramics, AGH University of Krakow, Krakow, Poland; [3]Jerzy Haber Institute of Catalysis and Surface Chemistry, Polish Academy of Sciences, Krakow, Poland; [4]Department of Geology, Geophysics and Environmental Protection, AGH University of Krakow, Krakow, Poland

Correspondence: Anna Rudawska, Email anna.rudawska@hirszfeld.pl

Introduction: Boron neutron capture therapy (BNCT) is a targeted radiotherapy that represents a promising treatment for glioblastoma multiforme. BNCT efficacy depends on selective boron carriers capable of crossing the blood–brain barrier (BBB). Therefore, we propose an original strategy for boron delivery in BNCT, based on the cellular carriers. This study assessed the ability of bone marrow-derived macrophages (BMDMs) to accumulate boron carbide (B_4C) nanoparticles, transport them across an in vitro BBB model toward glioblastoma cell-conditioned medium, and interact with tumor cells.

Methods: The uptake and accumulation of B_4C nanoparticles by BMDMs in different polarization states (M0, M1, M2) were confirmed by holotomography and ICP-MS. The scratch assay assessed spontaneous migration of BMDMs loaded with B_4C nanoparticles. The Transwell system was used to determine the ability of BMDMs with B_4C to cross bEnd.3 brain endothelial cell monolayer, mimicking the BBB, toward GL-261 glioblastoma cell-conditioned medium rich in CCL2. Macrophage interactions with glioblastoma spheroids were investigated using the CellTiter-Glo 3D Cell Viability Assay and flow cytometry.

Results: All BMDM populations demonstrated the ability to accumulate B_4C nanoparticles, with the significantly highest boron concentration detected in M1 macrophages (21.53 ± 1.64 mg/L per 10^6 cells). Moreover, M0, M1, and M2 macrophages loaded with B_4C nanoparticles were capable of migrating through the brain endothelial cell monolayer, toward the glioblastoma cell-conditioned medium. BMDMs with nanoparticles did not affect the viability of glioblastoma spheroids after 6 days of co-culture, in contrast to macrophages without nanoparticles, which increased the survival of tumor cells. Importantly, CD206 expression was not increased in M1 macrophages after contact with spheroids, and was lower in M2 macrophages loaded with B_4C nanoparticles compared to control M2 macrophages.

Conclusion: BMDMs are promising carriers of B_4C nanoparticles for BNCT due to their ability to cross the in vitro BBB model toward the glioblastoma microenvironment.

Keywords: macrophages, cellular carriers, boron carbide nanoparticles, blood-brain barrier, glioblastoma multiforme, boron neutron capture therapy

Introduction

Glioblastoma multiforme (GBM) is the most common malignant brain tumor in adults, accounting for approximately half of all primary tumors of the central nervous system.[1] GBM is a highly aggressive grade IV tumor with a poor prognosis. Standard treatment includes surgical resection supplemented with radiotherapy and temozolamide chemotherapy. However, due to treatment resistance, conventional therapies are not effective for many patients, resulting in frequent tumor recurrence and high mortality.[2,3] Treatment of GBM remains a significant challenge due to the tumor's location in hard-to-reach areas of

https://doi.org/10.2147/IJN.S604151
Received: 18 February 2026
Accepted: 8 May 2026
Published: 3 June 2026

Graphical Abstract

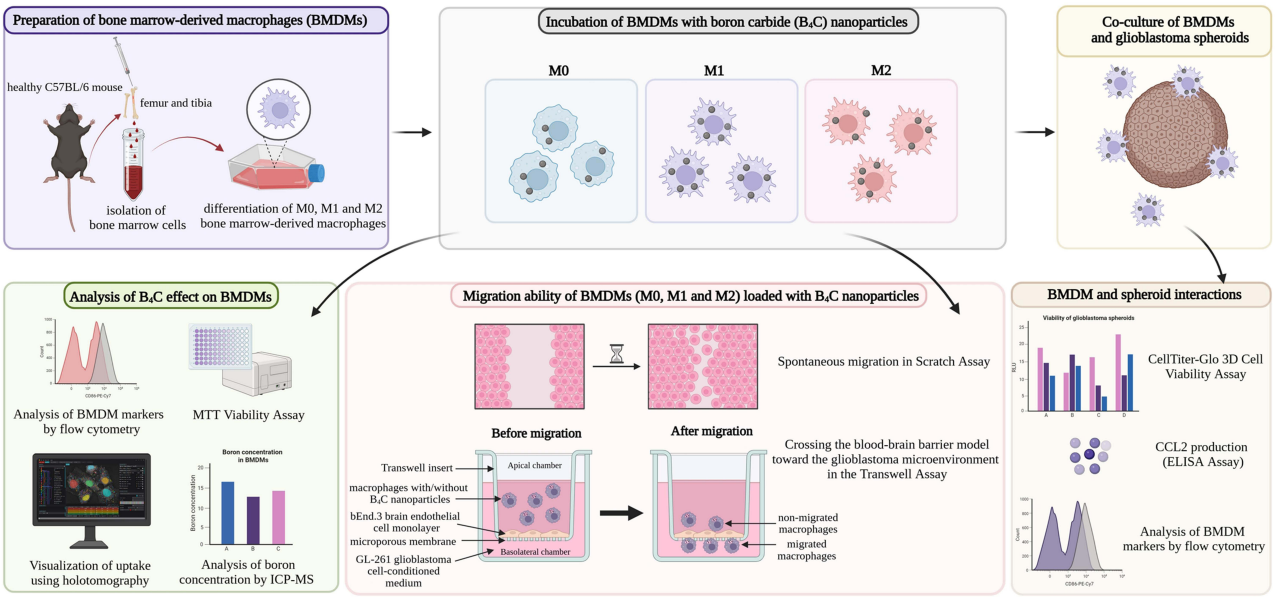

a crucial organ, its heterogeneous nature, the immunosuppressive tumor microenvironment (TME), and the presence of the blood-brain barrier (BBB), which is impenetrable to many drugs.[4]

The high resistance of GBM to conventional treatments increases the need for new effective therapies. One promising approach is boron neutron capture therapy (BNCT), which is a type of targeted radiotherapy that destroys tumors at the cellular level.[5] The basis of BNCT is irradiation of the tumor containing the accumulated boron-10 (^{10}B) isotope with thermal or epithermal neutrons. The reaction results in the emission of an alpha particle (^{4}He) and a recoiling lithium-7 nucleus (^{7}Li) with high linear energy transfer (LET), and gamma radiation. The released energy is deposited within a single tumor cell radius (<10 μm), limiting the destructive effect on normal cells. Therefore, BNCT was developed to treat patients with unresectable, recurrent, and locally advanced cancers such as GBM, head and neck cancers, and melanomas.[6]

Clinical trials of BNCT have been ongoing since the 1950s. Initially, the availability of nuclear reactors necessary to generate a neutron beam was a limitation. However, the development of accelerator technology has enabled the use of BNCT in hospitals.[5] In 2020, Japan became the first country to approve BNCT for the treatment of patients with head and neck cancer.[7] However, its use in GBM is still limited to clinical trials. The reason for the lack of widespread implementation of this therapy is the deficiency of boron carriers that selectively accumulate in cancer cells, providing the required boron concentrations (>20 μg ^{10}B per gram of tumor or > 10^{9} atoms per cell). Furthermore, boron carriers should be characterized by a lack of systemic toxicity, maintaining a constant boron concentration during neutron irradiation, as well as rapid clearance from the blood and normal tissues. Additionally, in the case of brain tumors, the ability to cross the BBB is necessary. Therefore, there is a great need to find a boron carrier that meets all the requirements.[8]

One of the promising candidates for BNCT is boron carbide (B_4C), characterized by high neutron absorptivity. Moreover, B_4C can form diverse stoichiometries with a high boron content.[9] In our previous work, we confirmed that originally synthesized boron carbide nanoparticles delivered a high concentration of boron (~7.8 mg/L of boron per 10^{6} cells) to cancer cells.[10] However, to increase the selectivity of delivery of this compound to the TME and reduce undesirable interactions with normal cells, the use of targeted delivery methods is crucial. For this purpose, we propose using a "Trojan horse" strategy based on macrophages as cellular carriers of boron carbide nanoparticles, which is an original approach to boron delivery in BNCT. Macrophages exhibit natural phagocytic abilities to engulf foreign particles, as well as low immunogenicity, biocompatibility, and long viability. Importantly, macrophages cross biological barriers, including the BBB, and due to

their tropism toward hypoxia, they efficiently migrate and accumulate in the TME[11] Encapsulation of nanoparticles within macrophages reduces their systemic toxicity and enables their selective delivery to the TME. Furthermore, in the case of brain tumors, it bypasses the requirements that nanoparticles must meet to effectively cross the BBB, such as a size of 10–1000 nm, a positive charge, a rod-like structure, and lipophilicity.[12]

In GBM, tumor-associated macrophages (TAMs) forming the TME may constitute 30–50% of the tumor mass. TAMs found in GBM originate from microglia present in the brain, but also from bone marrow-derived macrophages (BMDMs).[13] The main factor responsible for the migration and recruitment of monocytes and macrophages from the blood circulation to the brain tumor is C-C motif chemokine ligand 2 (CCL2), also known as monocyte chemotactic protein-1 (MCP-1). CCL2, abundantly produced by GBM cells, binds to the C-C chemokine receptor type 2 (CCR2) present on monocytes/macrophages and promotes their differentiation into TAMs.[14]

BMDMs present in TME possess diverse phenotypes and functions that are acquired in response to environmental stimuli due to their phenotypic plasticity. The main classification of macrophages includes classically activated macrophages (M1) and alternatively activated macrophages (M2), among which the following subpopulations are distinguished: M2a, M2b, M2c, and M2d.[15] M1 cells produce pro-inflammatory cytokines and chemokines such as IL-1α, IL-1β, IL-6, IL-12, and TNF-α, stimulating Th1 lymphocytes and participating in antitumor responses and inhibiting tumor progression. M1 macrophages present antigens via the major histocompatibility complex class II (MHC II) and also express the costimulatory molecules CD80 and CD86 on their surface.[16] M2 macrophages secrete anti-inflammatory cytokines (IL-4, IL-10, and IL-13), chemotactic and angiogenic factors, as well as extracellular matrix components, promoting tumor progression. M2 cells, creating an immunosuppressive TME, inhibit the action of cytotoxic T lymphocytes and attract regulatory T lymphocytes (Tregs) and myeloid-derived suppressor cells (MDSCs). Furthermore, M2 cells overexpress mannose receptors such as CD206 and CD209. Due to the immunosuppressive effect of the TME, M1 macrophages may undergo repolarization to the M2 phenotype, resulting in the predominance of M2 macrophages among TAMs.[13,17]

Macrophages have been shown to be effective as cellular carriers in GBM models, including the delivery of ferritin-protein cages[18] and doxorubicin nanoparticles.[19,20] The proposed strategy for using macrophages as boron carriers in BNCT represents an innovative and original approach. In our previous studies, we demonstrated a relationship between the polarization state of BMDMs (M0, M1, and M2) and their sensitivity to boron carbide nanoparticles.[21] We also confirmed the ability of all BMDM populations to effectively engulf and accumulate B_4C nanoparticles. To complement and extend these studies, the current work focuses on the crucial aspects of using BMDMs as boron carriers in BNCT. The main aim of this study was to quantify the uptake and accumulation of B_4C by BMDMs, determine the ability of these cells to transport B_4C across the in vitro BBB model and migrate toward glioblastoma cell-conditioned medium, and analyze macrophage interactions with tumor spheroids.

Materials and Methods

Boron Carbide Nanoparticles

Boron carbide (B_4C) nanoparticles used in this study were synthesized by the vapor deposition and had a size of 32 ± 10 nm. Detailed characterization of the obtained B_4C nanoparticles was performed using dynamic light scattering (DLS), laser Doppler velocimetry (LDV), atomic force microscopy (AFM), X-ray diffraction analysis (XRD), scanning electron microscope (SEM), and transmission electron microscope (TEM), as described in the work of Kozień et al.[22]

Cell Culture

Mouse bEnd.3 endothelial cells obtained from the American Type Culture Collection (ATCC; CRL-2299) were maintained in Dulbecco's modified Eagle's medium (DMEM; ATCC) containing 10% heat-inactivated fetal bovine serum (FBS; ATCC), 100 U/mL penicillin, and 100 mg/mL streptomycin (all from Sigma-Aldrich).

Mouse GL-261 glioblastoma cells obtained from the Leibniz Institute DSMZ (German Collection of Microorganisms and Cell Cultures GmbH; ACC 802) were maintained in DMEM (ATCC) supplemented with 10% FBS, 100 U/mL penicillin, and 100 mg/mL streptomycin (all from Sigma-Aldrich). All cell cultures were maintained in a NUAIRE CO_2 incubator (37°C, 5% CO_2, 95% humidity).

Preparation of Bone Marrow-Derived Macrophages

Laboratory animals used in this study were housed and handled in accordance with animal welfare principles set out in Directive 2010/63/EU of the European Parliament and of the Council and the Polish Act on the Protection of Animals Used for Scientific or Educational Purposes (Journal of Laws 2015, item 266).

Healthy 7–8 week old female C57BL/6 mice were euthanized by cervical dislocation in accordance with the guidelines of the above-mentioned Directive and Act. The femurs and tibias were then collected from the mice. To isolate bone marrow cells, the marrow cavities of the cleaned bones were flushed with RPMI-1640 medium (Gibco) supplemented with 3% FBS, 100 U/mL penicillin, and 100 mg/mL streptomycin (all from Sigma-Aldrich). Isolated bone marrow cells were centrifuged for 7 minutes at 192 × g at 4°C, and placed on T75 culture flasks (Corning). Cells were cultured in RPMI-1640 medium (Gibco) with the addition of 1 mM sodium pyruvate, 0.05 mM 2-mercaptoethanol, 10% FBS, 100 U/mL penicillin, 100 mg/mL streptomycin (all from Sigma-Aldrich), and 50 ng/mL recombinant mouse macrophage colony-stimulating factor (M-CSF; ImmunoTools), called culture medium. The medium was replaced with a fresh one every 2 days. After 8 days of culture under these conditions, unpolarized (M0) BMDMs were obtained. To activate macrophages, after 7 days of culture with M-CSF, 20 ng/mL interferon-γ (IFN-γ; ImmunoTools) and 100 ng/mL lipopolysaccharide (LPS, from E. coli O111:B4; Sigma Aldrich) were added for 24 hours to polarize to M1 macrophages, and 20 ng/mL interleukin 4 (IL-4; ImmunoTools) to polarize to M2 macrophages.

Phenotypic Characterization of BMDMs by Flow Cytometry

Phenotypic characterization was performed using flow cytometry to confirm the differentiation of bone marrow cells toward macrophages, their activation status, and the lack of influence of B_4C nanoparticles on antigen expression. Briefly, BMDMs were stained with cocktails of fluorochrome-conjugated monoclonal antibodies: anti-F4/80 Alexa Fluor 700, anti-CD11b PerCP-Cy5.5, anti-MHC II FITC, anti-CD86 PE-Cy7 (all from BioLegend), anti-CD40 PE (Becton Dickinson), and appropriate isotype controls. Then, the cells were fixed using the Foxp3/Transcription Factor Staining Buffer Set (Thermo Fisher Scientific) and incubated with anti-CD206 APC (BioLegend) antibody. Analysis was performed using an LSRFortessa flow cytometer with Diva Software (Becton Dickinson). The graphs and histograms were prepared in GraphPad Prism 10 (GraphPad Software) and NovoExpress 1.3.0 software (ACEA Biosciences, Inc). A detailed scheme of BMDM analysis was published in the work of Wróblewska et al.[21]

Additionally, to evaluate the influence of glioblastoma spheroids on changes in the expression of BMDM-specific antigens, phenotypic characterization was performed on days 3 and 6 of co-culture as described above. The only exception to the procedure was the separation of spheroids into single cells by adding 150 μL/well of LifeGel Digestion (RealResearch) for 10 minutes before staining with the antibody cocktail. The phenotypic characterization of BMDMs after 3 and 6 days of co-culture with glioblastoma spheroids was performed in two independent experiments.

Formation of Glioblastoma Spheroids

GL-261 cells were seeded at a density of 2×10^3 cells/well in 96-well plates coated with LifeGel (Real Research) in DMEM (ATCC) containing B-27 supplement (Gibco), 20 ng/mL epidermal growth factor (EGF; ImmunoTools), 20 ng/mL fibroblast growth factor (FGF; ImmunoTools), 100 U/mL penicillin, and 100 mg/mL streptomycin (Sigma-Aldrich). From day 6 of culture, the culture medium was replaced every 2 days to ensure spheroid growth.

Co-Culture of Glioblastoma Spheroids and BMDMs

On the 8th day of culture, M0, M1, and M2 macrophages, both with or without B_4C nanoparticles, were placed onto 10-day-old GL-261 spheroids at a density of 5×10^3 cells/well in RPMI-1640 medium (Gibco) supplemented with 10% FBS, 100 U/mL penicillin, and 100 mg/mL streptomycin (all from Sigma-Aldrich). Co-culture was conducted for 3 and 6 days at 37°C (5% CO_2, 95% humidity).

For fluorescence microscopy imaging, macrophages were stained with 2 μM Calcein AM Green (Thermo Fisher Scientific) before addition to spheroids. GL-261 spheroids with and without BMDMs were observed using an Olympus IX81 inverted fluorescence microscope.

MTT Cell Viability Assay

M0, M1, and M2 BMDMs were placed in 96-well plates at a density of 2×10^4 cells/well. After one day, boron carbide nanoparticles were added to a final concentration ranging from 0.1 to 400 μg/mL and incubated for 24 hours. MTT dye (3-(4,5-dimethylthiazol-2-yl)-2,5-diphenyltetrazolium bromide; Sigma-Aldrich) was then added at 5 mg/mL for 4 hours, followed by lysing overnight in lysis buffer (*N,N*-dimethylmethanamide, sodium dodecyl sulfate, and water) at 37°C. The absorbance of the dissolved formazan crystals was measured at 570 nm using a BioTek Epoch 2 plate reader with Gen5 Software (Agilent Technologies). MTT assays were performed in three independent experiments.

Holotomography

M0, M1, and M2 BMDMs were seeded on a TomoDish (Altium) at a density of 2×10^5 cells in 2 mL of culture medium. After attaching the cells to the dish, B_4C nanoparticles were added to a final concentration of 100 μg/mL for 24 hours. Afterwards, the culture medium containing noninternalized nanoparticles was removed and replaced with fresh medium. The cells were visualized with an HT-2H commercial optical diffraction tomography microscope (Tomocube Inc). Three-dimensional refractive index (RI) tomograms were created from a series of two-dimensional holographic images obtained from 49 illumination conditions. The diffracted beams from the samples were collected using a high numerical aperture (NA = 1.2) objective lens UPLSAP 60XW (Olympus). Data processing and visualization were performed with TomoStudio HT-2H Gen3-3.3.9 software (Tomocube Inc).

Analysis of the Boron Content in BMDMs Using ICP-MS

Preparation of Samples

M0, M1, and M2 BMDMs were placed in 24-well plates at a density of 2×10^5 cells/well. Next, boron carbide nanoparticles were added to a final concentration of 100 μg/mL and incubated for 24 hours. After this time, the medium above the cells was removed, and the cells were washed three times with phosphate-buffered saline (PBS). Proteinase K (Sigma-Aldrich) solution at a concentration of 1 mg/mL in 100 mM sodium bicarbonate (POCH) was then added and incubated for 30 minutes at 50°C. Cells were harvested from plates, and the wells were washed 2 times with MiliQ water to collect all cells.

Microwave Digestion of Samples

The samples under investigation had to be dissolved in a homogeneous solution before instrumental analysis. This process uses the modern ultraWAVE mineralization system (Milestone Srl). First, the material was well-mixed using a vortex mixer. Approximately 0.5 g of each material was sampled and placed into Teflon vessels, followed by the addition of 5 mL of concentrated 67% ultrapure nitric acid (V) (NORMATOM, Ultrapure for trace metal analysis). The vessels were subsequently positioned in a microwave mineralizer. The mineralization procedure involved heating to 250°C over 25 minutes and maintaining the target temperature for 20 minutes, with the microwave power set to 1500 W. After digestion, the resulting solutions were quantitatively transferred to 10 mL polypropylene vessels (borosilicate glassware was avoided to prevent boron contamination) and diluted to a final mass of 10 g with deionized water obtained from the Direct-Q 3 UV system (Merck Millipore). The prepared solutions were then subjected to instrumental analysis to determine the total boron concentration in the samples.

Instrumental Analysis of the Boron Content by ICP-MS

After microwave digestion, samples containing BMDMs both with and without boron carbide nanoparticles were analyzed using the inductively coupled plasma mass spectrometry (ICP-MS) technique on the iCAP RQ (C2) instrument (Thermo Fisher Scientific) in accordance with the ISO 17294–2 standard.[23] A five-point calibration curve, including a blank, was prepared for the analysis, covering concentrations ranging from 5 to 500 μg/L. Both the certified boron reference materials applied for calibration and the laboratory control samples used to verify the calibration curve were produced in accordance with ISO 17034 standards.[24] The certified reference materials used were Boron B - 10 g/L in H_2O for ICP (CPAchem Ltd) and ICP multielement standard solution IV (Supelco Analytical Products). Quantitative determination was carried out using the isotope ^{10}B, which occurs naturally at about 20% abundance. Based on the measurements, the estimated limit of

quantification was 1 μg/L, while the uncertainty associated with boron determination by ICP-MS was 16%. Final results were corrected for the sample mass subjected to mineralization and the diluted final mass. Measurements were performed on three independent biological samples for each macrophage population. Taking into account the number of cells and the boron content in the sample, the boron concentration per 10^6 cells was calculated.

Scratch Assay

M0, M1, and M2 BMDMs were placed at a density of 8×10^5 cells/well in 6-well plates in the culture medium. B_4C nanoparticles at a final concentration of 100 μg/ mL were added for 24-hour incubation. Next, a gentle scratch was made with a 200 μL tip in the center of the cell monolayer in the wells. The floating cells were removed by washing with PBS, and then the culture medium was added. The macrophages were incubated at 37°C (5% CO_2, 95% humidity) and imaged over time for 24 hours using an Olympus CKX53 light microscope. Two independent experiments were performed. The images show a selected part of the well for each sample at 0, 4, and 24 hours.

Determination of CCL2 Production

Conditioned medium was collected from adherent GL-261 cell cultures after 24, 48, and 72 hours, and after 3 and 6 days of co-culture of BMDMs with GL-261 spheroids. The concentration of CCL2 was determined using a commercially available ELISA kit (Invitrogen). The test was conducted according to the manufacturer's instructions, with each sample tested in triplicate.

Transwell Migration Assay

To generate a monolayer of brain endothelial cells imitating the blood-brain barrier, 7.5×10^4 bEnd.3 cells were placed on Transwell inserts (pore size: 3 μm; Corning) in 150 μL of DMEM supplemented with 10% FBS, 100 U/mL penicillin, and 100 mg/mL streptomycin per insert, and placed in a 24-well plate. After 3 days, the culture medium on the inserts was replaced with fresh medium. On day 5 of bEnd.3 cell culture on the inserts, after a compact monolayer had been achieved and a transepithelial electrical resistance (TEER) of at least 20 $\Omega\cdot cm^2$ had been reached, the Transwell migration assay was initiated. This TEER value is typical of the bEnd.3 cell monolayer and is expressed after subtracting the TEER for blank inserts. TEER was measured using Millicell ERS-2 (Merck Millipore).

M0, M1, and M2 macrophages were incubated with boron carbide nanoparticles at a concentration of 100 μg/mL for 24 hours. Next, all macrophage populations, both with and without B_4C nanoparticles at a density of 5×10^4 cells/insert, were applied to the bEnd.3 cell-coated inserts in 150 μL of RPMI-1640 medium supplemented with 1 mM sodium pyruvate, 0.05 mM 2-mercaptoethanol, 100 U/mL penicillin, and 100 mg/mL streptomycin. Two additional inserts were also prepared with only a monolayer of bEnd.3 cells adding only medium without BMDMs, as a "blank" and as a control monolayer coating the insert. A 72-hour GL-261 cell-conditioned medium was added to the lower chambers. After 18 hours of incubation at 37°C (5% CO_2, 95% humidity), the upper part of the inserts was wiped using a cotton swab to remove cells that did not migrate, except for the monolayer control insert, which was not wiped off. Then, the cells on the inserts were stained with the RAL 555 kit (RAL Diagnostics) according to the manufacturer's instructions. Migrated cells were observed by an Olympus CKX53 light microscope and counted using ImageJ software from 6 images of the central part of each insert. The migration assay was performed in two independent experiments.

CellTiter-Glo 3D Cell Viability Assay

To determine the effect of BMDMs on the viability of glioblastoma spheroids after 3 and 6 days of co-culture, CellTiter-Glo 3D reagent (Promega) was added and incubated for 30 minutes in the dark at room temperature. After this time, the relative luminescence units (RLU) were measured using the BioTek Synergy H4 plate reader with Gen5 Software (Agilent Technologies) and an integration time of 0.5 s. The RLU values for the corresponding macrophage populations were subtracted from the RLU values obtained for the co-cultures to obtain the RLU value of glioblastoma spheroids. The CellTiter-Glo 3D cell viability assay was performed in two independent experiments.

Statistical Analysis

All data were analyzed using GraphPad Prism 10 software (GraphPad Software). The D'Agostino−Pearson omnibus test confirmed the normality of residuals. When the data were consistent with a Gaussian distribution and had equal standard deviation (SD) values, statistical significance was calculated using the parametric one-way ANOVA or the two-way ANOVA followed by Tukey's multiple comparison post-hoc test. When data were consistent with a Gaussian distribution, but SD values were not equal, the Brown−Forsythe and Welch ANOVA test, followed by Dunnett's T3 multiple comparisons post-hoc test, was performed. The type of statistical analysis used is described in the captions under the figures. All statistically significant differences are presented in graphs when $p<0.05$; otherwise, the differences were not significant.

Results

Effect of B_4C Nanoparticles on the Viability and Phenotype of BMDMs

To develop effective cellular carriers, it is crucial to select the nanoparticle concentration that does not affect cell viability, mobility and phenotype. Therefore, in the first stage of the study, the effect of boron carbide nanoparticles on the viability of M0, M1, and M2 BMDMs after 24 hours of exposure was assessed using the MTT assay (Figure 1A). The results demonstrated boron carbide toxicity toward BMDMs only at higher concentrations above 100 μg/mL, with M1 macrophages being the most sensitive population to B_4C nanoparticles. The concentration of 100 μg/mL was selected as optimal for further studies, because it did not reduce macrophage viability below 70%.

Additionally, phenotypic characterization was performed on day 8 of BMDM culture without boron carbide nanoparticles and after 24-hour exposure to 100 μg/mL B_4C (Figure 1B). Macrophages were characterized as F4/80 and CD11b positive cells using flow cytometry. Expression of markers such as MHC II, CD40, and CD86 was determined in the BMDMs in three polarization states (M0, M1, and M2). The highest expression of all antigens was observed in M1 macrophages. Furthermore, the obtained results showed that boron carbide nanoparticles had no significant effect on the mean fluorescence intensity (MFI) of all markers. This confirms the stability of the macrophage phenotype after 24-hour incubation with B_4C nanoparticles at a selected concentration.

Uptake and Accumulation of B_4C Nanoparticles in BMDMs

In the next stage, the uptake of boron carbide nanoparticles by M0, M1, and M2 BMDMs was compared. For this purpose, BMDMs were incubated for 24 hours with B_4C nanoparticles at a concentration of 100 μg/mL. Initially, macrophages with accumulated nanoparticles were visualized using holotomographic microscopy (Figure 2). Three-dimensional (3D) images were generated using a pseudo-coloring technique based on differences in refractive index (RI). In the 3D visualizations, green color indicates cell components (organelles, cytoplasm) that exhibit a lower RI (<1.4) than the boron carbide nanoparticles (RI>1.4), which are marked in red. Boron carbide nanoparticles were observed within all macrophage populations, but the highest accumulation was identified in M1 macrophages.

After an initial qualitative assessment of uptake, inductively coupled plasma mass spectrometry (ICP-MS) was used to quantitatively analyze the boron concentration engulfed by BMDMs (Figure 3). The analysis showed statistically significant differences in boron concentrations in all macrophage populations after incubation with B_4C nanoparticles compared to untreated cells, where the boron content was negligible (<0.35 mg/L per 10^6 cells). The highest boron concentration was detected in M1 macrophages (21.53 ± 1.64 mg/L per 10^6 cells), while the concentrations in M0 and M2 macrophages were 14.27 ± 1.36 mg/L and 16.72 ± 1.93 mg/L per 10^6 cells, respectively. The highest accumulation of boron carbide nanoparticles in M1 macrophages was associated with the greatest observed decrease in the viability of these cells among all BMDM populations.

Migration Ability of BMDMs

Another key aspect of effective cellular carriers is their ability to deliver engulfed nanoparticles to the target site. Therefore, the spontaneous migration ability of three macrophage populations (M0, M1, and M2) with and without accumulated boron carbide nanoparticles was compared using the scratch assay (Figure 4). The progress of cell migration was observed under

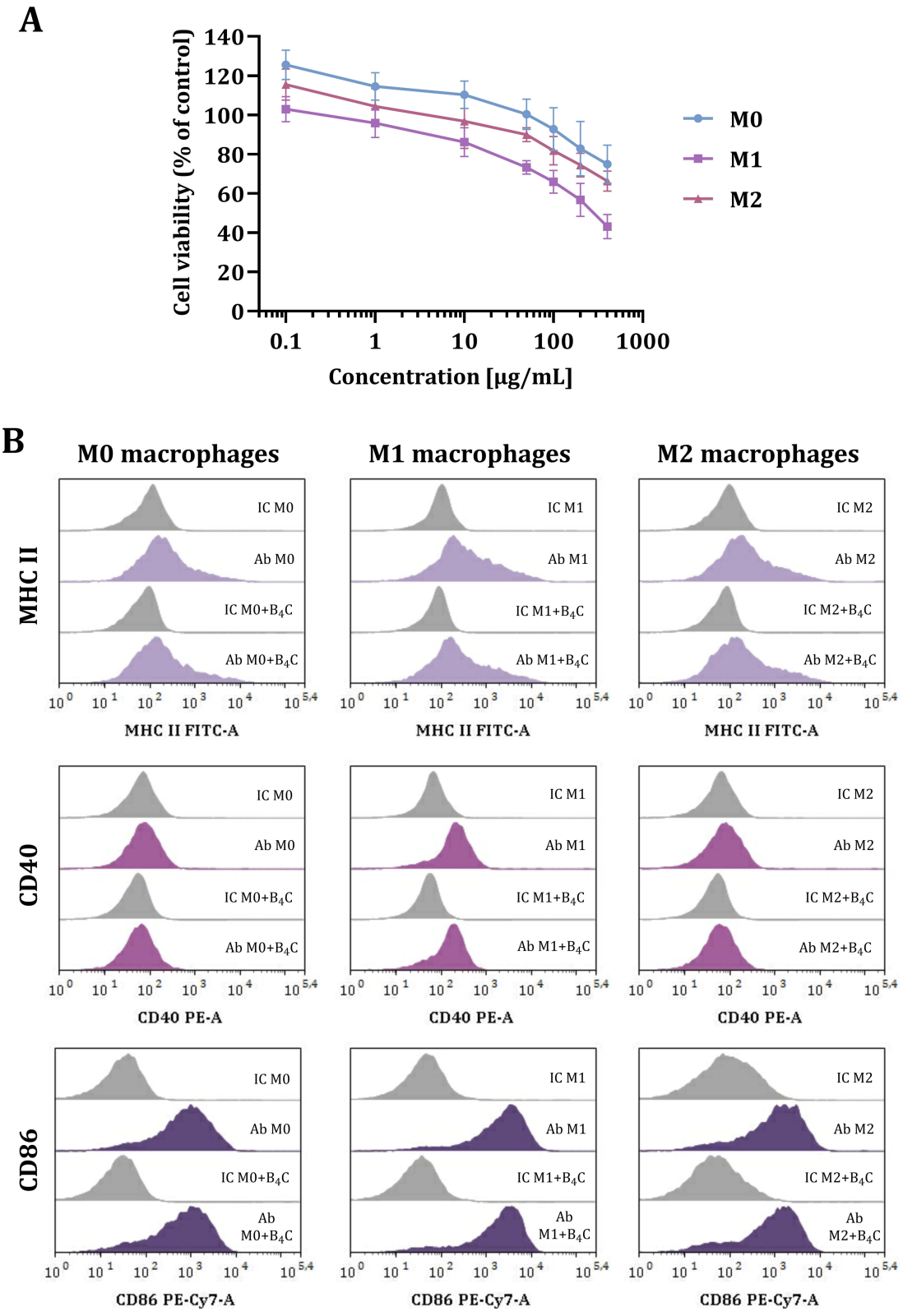

Figure 1 Effect of boron carbide nanoparticles on BMDMs in three polarization states (M0, M1, M2). (**A**) MTT viability assay on M0, M1, and M2 macrophages after 24-hour exposure to B_4C nanoparticles. The graph represents the percentage of viable cells relative to untreated control cells (control = 100%). The results are expressed as the means ± SD calculated for three independent experiments. (**B**) The phenotypic characterization of M0, M1, and M2 macrophages after 24-hour exposure to B_4C nanoparticles. Histograms show the mean fluorescence intensity (MFI) of the markers: MHC II, CD40, and CD86 in three populations of BMDMs ($F4/80^+CD11b^+$) with and without B_4C nanoparticles. The MFI value for each marker after antibody (Ab) staining is compared with the MFI value of the corresponding isotype controls (IC).

https://doi.org/10.2147/IJN.S604151

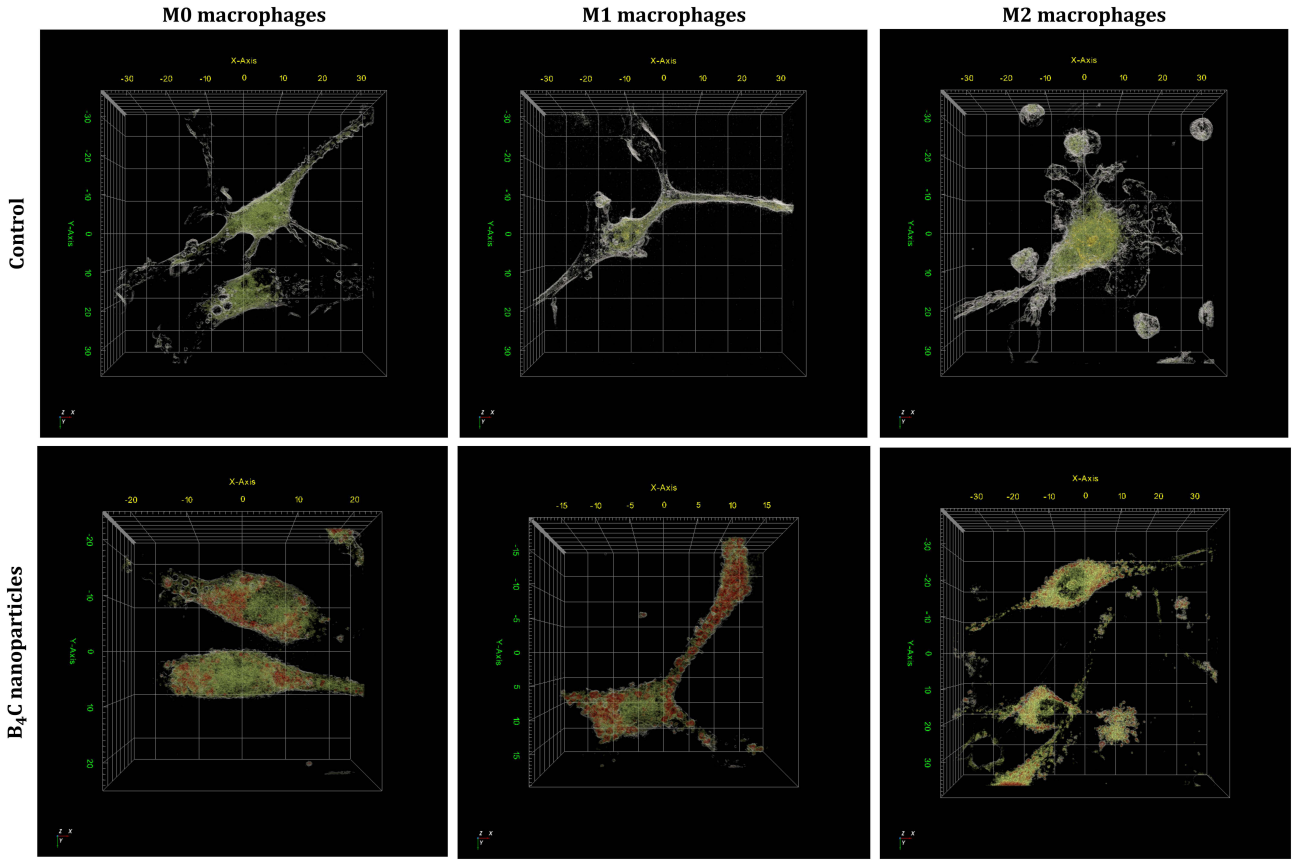

Figure 2 Three-dimensional holotomographic visualization of M0, M1, and M2 BMDMs with accumulated boron carbide nanoparticles compared to untreated cells, using pseudo-coloring based on refractive index (RI) ranges. Green structures have an RI of up to 1.4 and mark the interior of the cells (cytoplasm and organelles), while the red color corresponds to boron carbide nanoparticles with an RI above 1.4.

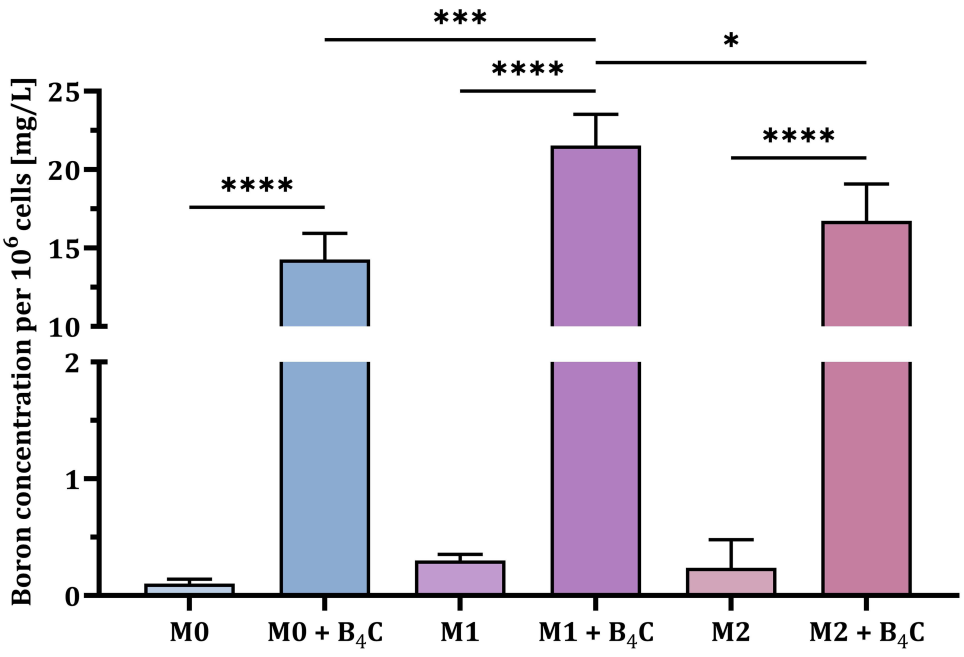

Figure 3 Boron concentration per 10^6 BMDMs in three populations (M0, M1, and M2) after 24 hours of incubation with boron carbide nanoparticles compared to untreated control cells. The results are expressed as the means + SD calculated from three independent biological samples. The differences between groups were calculated using the one-way ANOVA followed by Tukey's multiple comparison post-hoc test (*$p < 0.05$; ***$p < 0.001$; ****$p < 0.0001$).

https://doi.org/10.2147/IJN.S604151

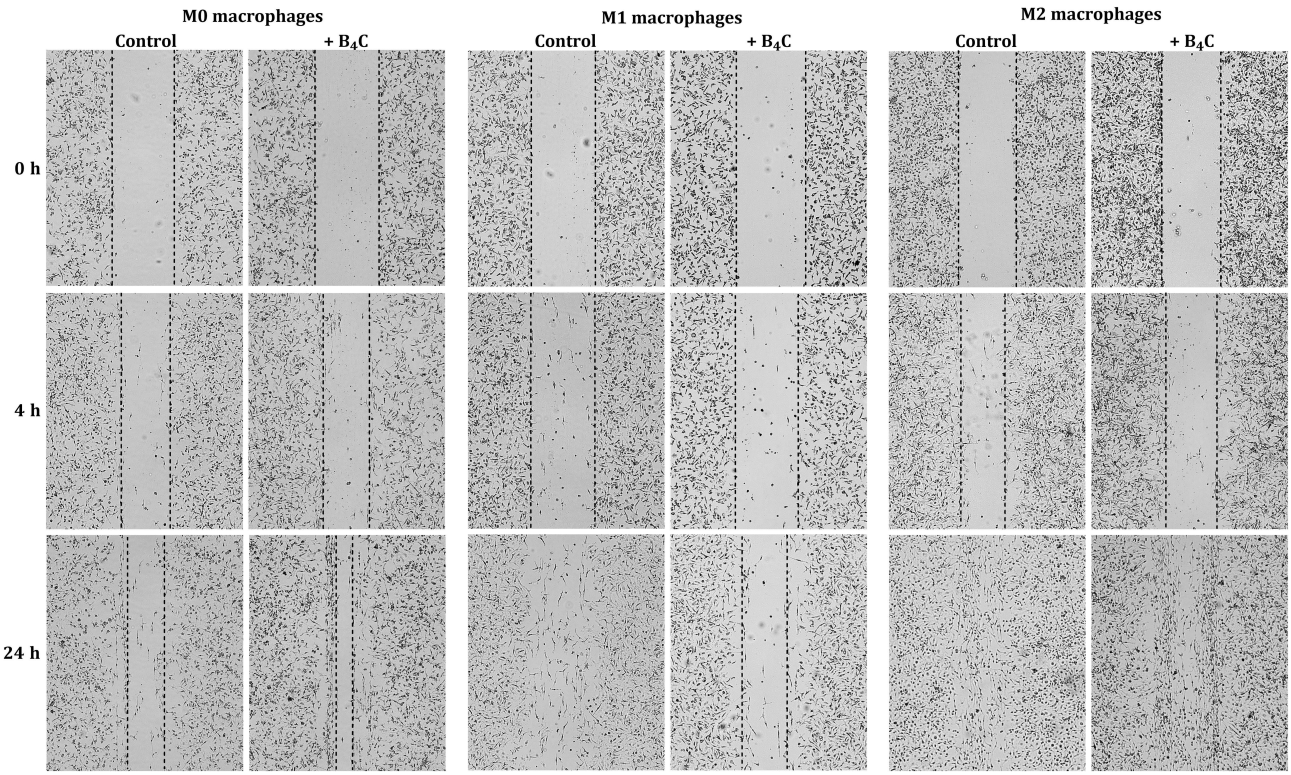

Figure 4 Assessment of the spontaneous migration ability of M0, M1, and M2 BMDMs with and without engulfed boron carbide nanoparticles based on the scratch assay after 4 and 24 hours.

a light microscope after 4 and 24 hours. The results showed that M0 macrophages migrated faster with B_4C nanoparticles than without them. In contrast, M1 macrophages with nanoparticles migrated more slowly than those without nanoparticles. The migration rate of M2 macrophages was the same regardless of the presence of nanoparticles. These observations indicate that efficient B_4C uptake by M1 macrophages affects not only their viability but also their mobility.

Crossing the in vitro BBB Model by BMDMs

In the case of brain tumors, the ability of the cellular carriers to cross the BBB is crucial. To compare the ability of three BMDM populations with and without accumulated boron carbide nanoparticles to migrate across the in vitro BBB model toward the GL-261 cell-conditioned medium, a Transwell migration assay was performed. First, the concentration of the chemokine CCL2 in the 24-, 48-, and 72-hour conditioned medium was assessed by ELISA due to its important role in macrophage recruitment to the TME (Figure 5A). The results showed the highest concentration of CCL2 in 72-hour GL-261 cell-conditioned medium at approximately 112 pg/mL and it was selected as a chemoattractant for the Transwell migration assay.

To create an in vitro model of the BBB, bEnd.3 brain endothelial cells were used to coat Transwell inserts. Then, M0, M1, and M2 BMDMs, both with and without accumulated boron carbide nanoparticles, were applied to an insert coated with endothelial cells (apical chamber). The wells under the inserts (basolateral chamber) were filled with 72-hour GL-261 cell-conditioned medium (Figure 5B). Inserts coated with endothelial cells without added BMDMs served as a control for bEnd.3 cell migration (blank) and as a control for monolayer integrity.

After 18 hours of migration, the migrated macrophages on the inserts were stained. The observations obtained in the Transwell test were similar to those in the scratch assay. The number of migrated M0 macrophages with B_4C nanoparticles was greater than that of M0 macrophages without nanoparticles (Figure 5C and D). M1 macrophages without B_4C nanoparticles migrated better than with nanoparticles. For M2 macrophages, both with and without nanoparticles, the number of migrated cells was similar. However, no statistically significant differences were found in the migration ability between M0, M1, and M2 macrophages loaded with nanoparticles.

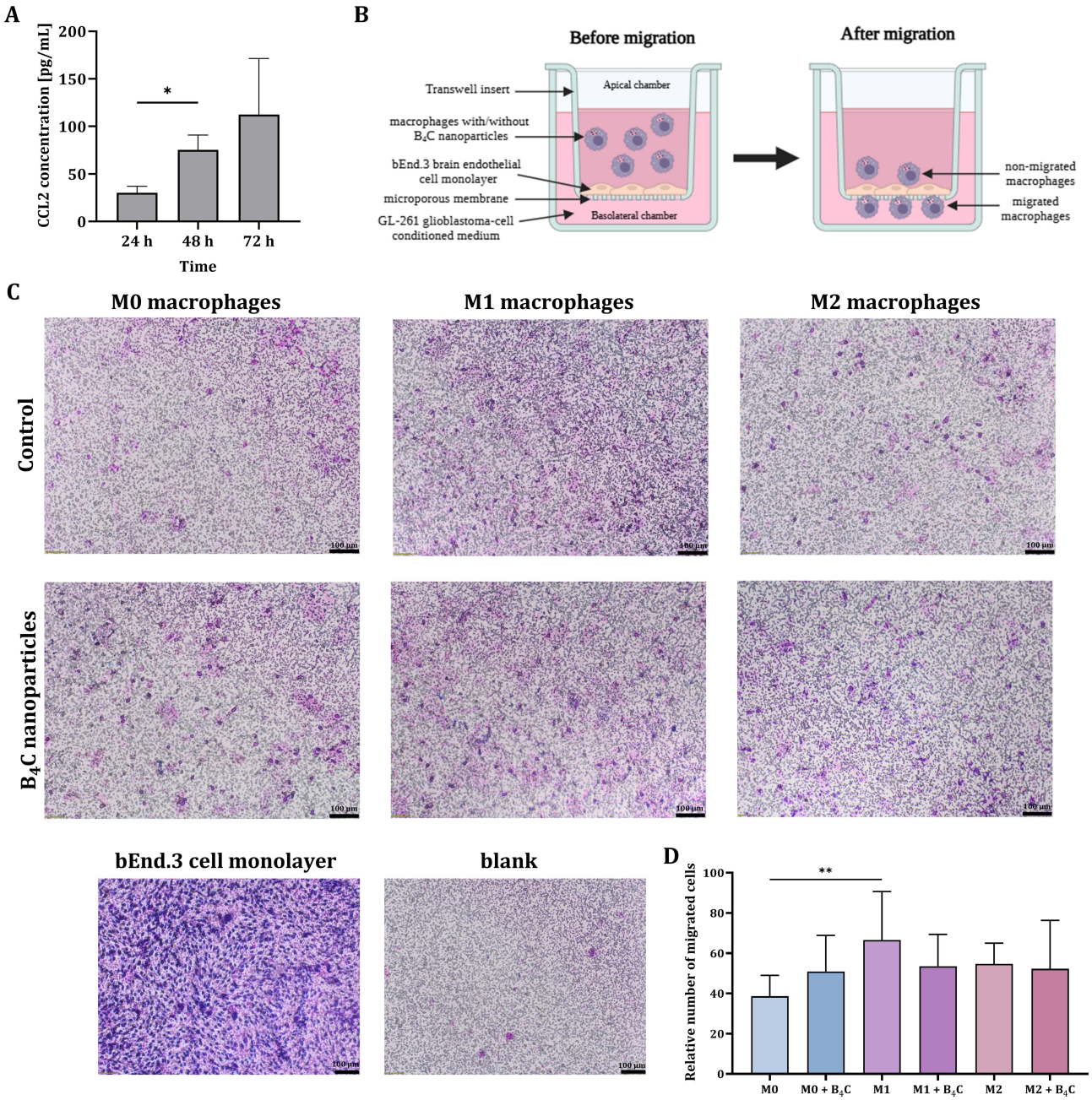

Figure 5 (**A**) CCL2 concentrations in 24, 48, and 72-hour GL-261 cell-conditioned medium determined by ELISA. (**B**) Schematic representation of the Transwell migration assay. (**C**) Images of migrated M0, M1, and M2 BMDMs with and without accumulated boron carbide nanoparticles through a bEnd.3 brain endothelial cell monolayer toward 72-hour GL-261 cell-conditioned medium containing CCL2. (**D**) Comparison of the average number of migrated cells counted from 6 images of the central part of each insert. The results are expressed as the means + SD calculated from two independent experiments. Differences between groups were calculated using the Brown–Forsythe and Welch ANOVA test, followed by Dunnett's T3 multiple comparisons post-hoc test (*$p < 0.05$) for CCL2 concentration data, and one-way ANOVA followed by Tukey's multiple comparison post-hoc test (**$p < 0.01$) for the number of migrated cells.

Effect of BMDMs on the Viability of GL-261 Spheroids and Changes in CCL2 Production in Co-Culture

The proven ability of BMDMs loaded with B_4C nanoparticles to cross the brain endothelial cell monolayer, mimicking the BBB, constitutes their advantage as cellular carriers. Therefore, subsequent steps were focused on assessing possible interactions between macrophages and tumor cells using 3D cultures. For this purpose, 10-day-old GL-261 spheroids

https://doi.org/10.2147/IJN.S604151

were co-cultured with three BMDM populations (M0, M1, and M2), with or without accumulated boron carbide nanoparticles. Control spheroid culture formed from GL-261 cells and co-culture with Calcein AM Green-labeled macrophages were imaged using a fluorescence microscope (Figure 6A). Co-culture of spheroids and BMDMs was conducted for 3 and 6 days. After this time, the effect of macrophages on spheroid viability was assessed using the CellTiter-Glo assay, in which relative luminescence units (RLU) correspond to cell viability (Figure 6B). After 3 days, a slight increase in the viability of glioblastoma spheroids was observed in co-cultures with macrophages loaded or unloaded with B_4C nanoparticles compared to control spheroids. However, after 6 days of co-culture, a differential survival of tumor cells was demonstrated. Importantly, macrophages loaded with nanoparticles did not affect spheroid viability, whereas contact with control macrophages increased the survival of glioblastoma cells.

Additionally, CCL2 levels were assessed in co-cultures of BMDMs and GL-261 spheroids after 3 and 6 days using ELISA (Figure 6C). The results showed higher CCL2 production after 6 days than after 3 days, both in co-culture and in the culture of macrophages and spheroids alone. After 3 days of culture, M1 macrophages loaded with B_4C nanoparticles produced less CCL2 than M1 without nanoparticles. The same tendency was also observed in co-culture with spheroids. However, in M0 and M2 populations, the effect was reversed. After 6 days of culture, M0, M1, and M2 macrophages loaded with B_4C nanoparticles produced more CCL2 than those without nanoparticles. When spheroids were co-cultured with nanoparticle-loaded M0 and M1 macrophages, CCL2 levels were lower than in co-cultures with BMDMs without engulfed nanoparticles. M2 macrophages with and without accumulated nanoparticles produced the highest levels of CCL2 among all populations, which was also observed in the CCL2 levels in co-culture with spheroids.

Effect of GL-261 Spheroids on Changes in the Phenotype of BMDMs

After 3 and 6 days of co-culture, the effect of GL-261 spheroids on changes in macrophage marker expression was assessed. For this purpose, the phenotypic characterization of three BMDM populations with and without accumulated boron carbide nanoparticles was performed using flow cytometry (Figure 7). The expression of MHC II and CD40 on the surface of M0, M1, and M2 macrophages increased after contact with spheroids at both time points, with the highest levels of these molecules found in the M1 population. However, increases in marker expression were greater in all unloaded macrophage populations than in nanoparticle-loaded cells. No statistically significant differences in MHC II and CD40 surface expression between days 3 and 6 of culture were observed.

At the second time point, both in culture with and without spheroids, a decrease in CD86 expression was observed in all macrophage populations. However, regardless of B_4C loading, M1 macrophages showed the highest expression of this molecule compared to the other populations.

After 6 days of culture, differences in mannose receptor expression levels were observed. In M0 macrophages, both with and without nanoparticles, an increase in CD206 expression was noted compared to control M0 macrophages. In M2 macrophages loaded with B_4C nanoparticles, CD206 expression was lower compared to M2 macrophages without nanoparticles. Meanwhile, the presence of tumor spheroids did not cause repolarization of M1 macrophages towards the M2 phenotype, as evidenced by the stable expression of CD206 not only on day 6 but also on day 3 of co-culture.

Discussion

The use of macrophages as cellular carriers in boron neutron capture therapy is an original and innovative strategy. In our previous work,[21] we demonstrated the potential of macrophages originating from a cell line and BMDMs to accumulate two boron carbide preparations differing in nanoparticle size. To continue and extend our research, we selected smaller nanoparticles (~32 nm), which showed less toxicity to macrophages than larger ones (~80 nm). Furthermore, we focused on BMDMs, which, as primary cells, better mimic in vivo macrophage physiology than those derived from cell lines.

To ensure efficient migration of macrophages to the target site, it is important to minimize the impact of engulfed compounds on their viability, phenotype, and normal function. Therefore, based on the MTT viability assay, we selected a B_4C nanoparticle concentration of 100 μg/L for further studies, which provides a high level of boron without significant toxicity during 24-hour incubation with BMDMs (Figure 1A). We also confirmed that this concentration did not influence changes in the expression of MHC II, CD40, and CD86 molecules on the surface of all macrophage populations after 24 hours of exposure (Figure 1B). Moreover, in previous studies, we demonstrated no changes in the production of

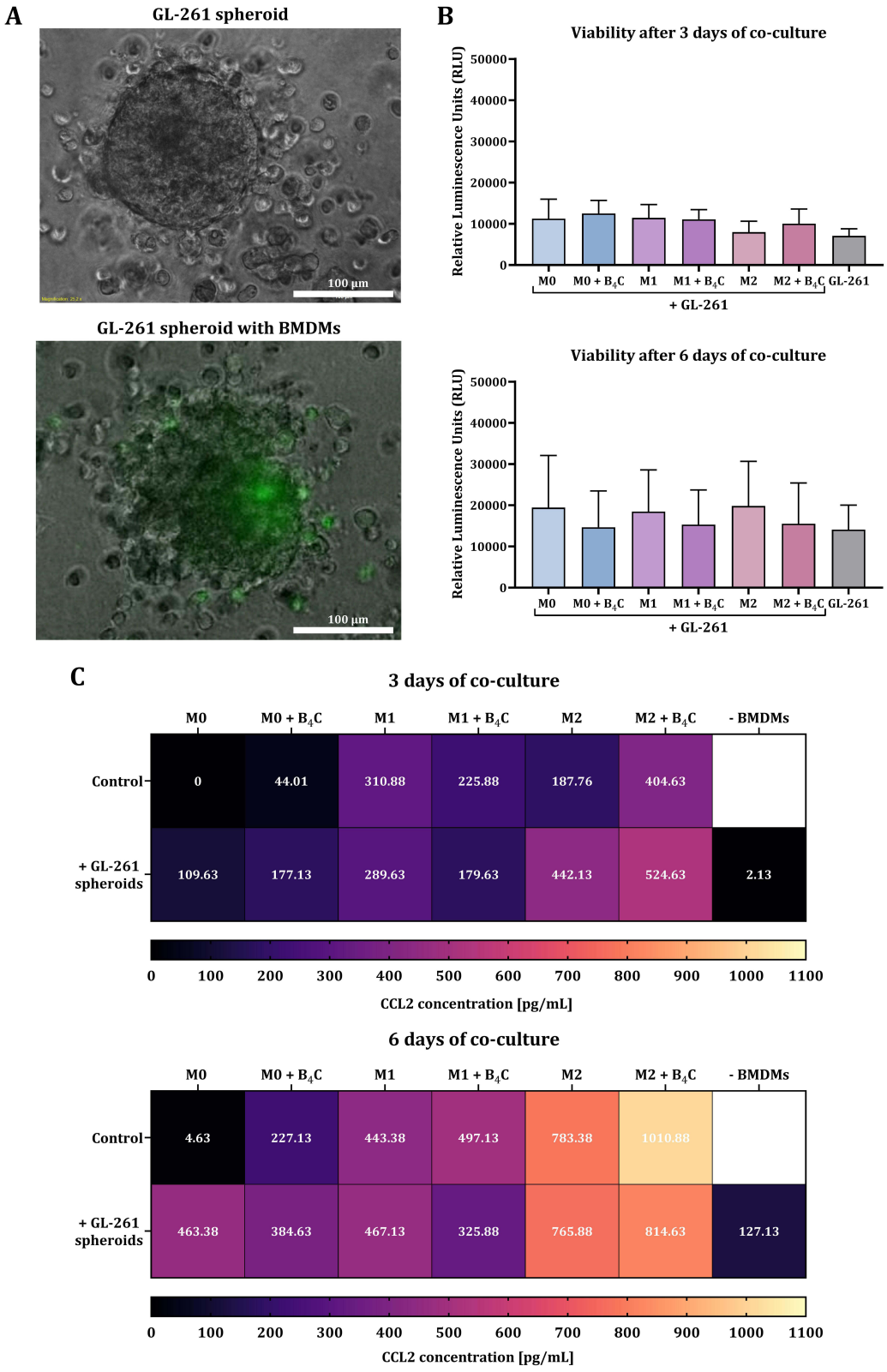

Figure 6 Effect of M0, M1, and M2 BMDMs loaded with or without boron carbide nanoparticles on the spheroids obtained from GL-261 glioblastoma cells after 3 and 6 days of co-culture. (**A**) Brightfield image showing a glioblastoma spheroid. Green fluorescence indicates BMDMs labeled with Calcein AM Green. (**B**) Viability of GL-261 spheroids determined by CellTiter-Glo 3D assay after 3 and 6 days of co-culture. The relative luminescence units (RLU) were obtained from GL-261 spheroids after subtracting the RLU value for the corresponding control macrophage population. The results are expressed as the means + SD calculated from two independent experiments. (**C**) Concentration of CCL2 in co-culture of glioblastoma spheroids with BMDMs after 3 and 6 days, compared to the production by macrophages and spheroids alone.

https://doi.org/10.2147/IJN.S604151

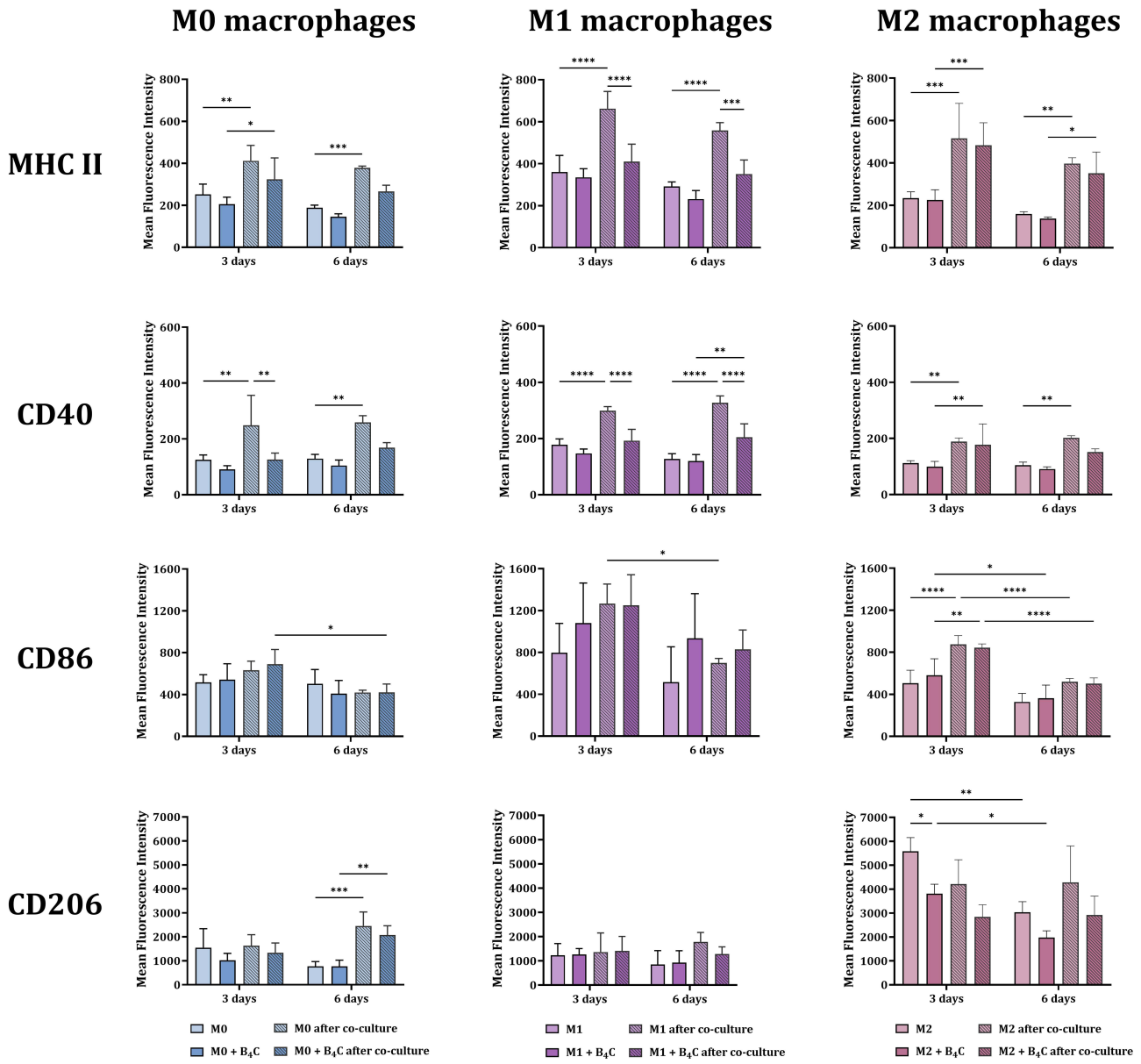

Figure 7 Phenotypic characterization of BMDMs loaded with or without boron carbide nanoparticles after 3 and 6 days of co-culture with glioblastoma spheroids. The mean fluorescence intensity of markers: MHC II, CD40, CD86, and CD206 was determined for the BMDM population ($F4/80^+CD11b^+$). The results are expressed as the means + SD calculated from two independent experiments. Differences between groups were calculated using two-way ANOVA followed by Tukey's multiple comparison post-hoc test (*$p < 0.05$; **$p < 0.01$; ***$p < 0.001$; ****$p < 0.0001$).

cytokines such as IL-1β, IL-6, IL-10, and TNF-α by all macrophage populations after incubation with B_4C nanoparticles at a concentration of 100 μg/mL.[21]

Another key aspect for obtaining cellular carriers is the effective internalization of the compound by macrophages. Therefore, we proved the uptake of boron carbide nanoparticles by M0, M1, and M2 macrophages over a 24-hour incubation period. Holotomographic microscopy visualization and ICP-MS analysis confirmed significant accumulation of nanoparticles in all macrophage populations (Figures 2 and 3). The highest boron concentration was detected in M1 macrophages. This may be due to the greater ability of activated M1 macrophages to phagocytize large amounts of particles compared to M0 and M2 macrophages. Moreover, it is related to the natural function of M1 macrophages in the immune response, which involves phagocytizing pathogens and presenting antigens to activate T helper 1 cells.[25] The differential ability of M0, M1, and M2 macrophages to accumulate nanoparticles observed in our study corresponds to other published results obtained for murine

BMDMs. In a study by Pang et al, M1 BMDMs demonstrated a significantly higher capacity to engulf doxorubicin-loaded poly(lactide-co-glycolide) (PLGA) nanoparticles compared to M0 macrophages.[20] Similarly, Qie et al showed that M1 macrophages had the highest ability to phagocytose carboxylic acid-terminated fluorescently labeled polystyrene nanoparticles compared to M0 and M2 macrophages.[26] Furthermore, Müller et al proved that M1 macrophages had higher phagocytic activity toward rabbit IgG-coated latex particles than M0 and M2 macrophages.[27]

The next important step in the development of cellular carriers was the assessment of the ability of macrophages loaded with boron carbide nanoparticles to spontaneously migrate and transport boron toward glioblastoma cell-conditioned medium. Based on the scratch assay, it was confirmed that among all macrophage populations with engulfed B_4C nanoparticles, M2 macrophages are characterized by the highest mobility (Figure 4). In contrast, M1 macrophages loaded with nanoparticles migrated the slowest. Similarly, in the work of Li et al, based on the calculated random motility coefficient, M2 BMDMs showed the highest migration ability compared to M0 and M1 macrophages.[28] This commonly observed phenomenon is related to stronger adhesion properties of M1 macrophages, which reduces their overall motility, while M2 macrophages have a more dynamic and less adherent migration profile.[29] This is due to the physiological functions of these phenotypically distinct macrophage populations. M2 macrophages play a crucial role in relieving inflammation and initiating the tissue repair process, in which migration to sites of injury is essential. The strong adhesion and limited motility of M1 macrophages allow them to accumulate at the site of inflammation, release inflammatory mediators, and eliminate pathogens.[30] Moreover, in this work, the slowest migration of M1 macrophages may be associated with the most efficient uptake of B_4C nanoparticles, as confirmed by the ICP-MS results.

The natural ability of macrophages to cross the BBB makes them extremely attractive cellular carriers for brain tumor therapies. However, to demonstrate that BMDMs loaded with B_4C nanoparticles can cross the in vitro BBB model, we used the Transwell system. For this purpose, we coated Transwell inserts with bEnd.3 brain endothelial cells, which form tight junctions with strong intercellular barrier properties.[31] As a chemoattractant, we utilized the 72-hour GL-261 cell-conditioned medium, which was rich in CCL2 (Figure 5A). The Transwell assay results correlated with the scratch assay observations. In the case of M0 macrophages, B_4C stimulated migration, whereas in M1 macrophages, it slightly inhibited migration compared to control macrophages (Figure 5C and D). A similar phenomenon was observed by Pang et al, who showed that doxorubicin-loaded PLGA nanoparticles reduced the migratory ability of M1 BMDMs through a monolayer of human umbilical vein endothelial cells (HUVECs) toward human U87 glioblastoma cells in a Transwell model.[20] Nonetheless, our results confirmed that all macrophage populations (M0, M1, and M2) loaded with boron carbide nanoparticles showed a similar ability to migrate through the endothelial cell monolayer toward the GL-261 cell-conditioned medium.

To assess the further fate of macrophages after crossing the in vitro BBB model, interactions between macrophages and glioblastoma spheroids, reflecting the TME, were analyzed. After 3 days of co-culture, all macrophage populations with and without nanoparticles slightly increased the viability of spheroids (Figure 6B). However, after 6 days, macrophages with accumulated B_4C showed no effect on tumor cell survival. While control BMDMs increased spheroid viability. The ability of macrophages in different polarization states (M0, M1, and M2) to stimulate the growth of tumor spheroids was also described by Francois et al[32] The lack of increased survival of glioblastoma cells under the influence of nanoparticle-loaded macrophages is a very beneficial phenomenon for the effectiveness of the proposed therapeutic strategy.

Considering the crucial role of CCL2 in the recruitment of monocytes and macrophages to the TME, its concentration was assessed in co-cultures of macrophages with glioblastoma spheroids. The observed significant increase in CCL2 production in all macrophage-spheroid co-cultures after 6 days, compared to day 3, may not only act as a positive feedback loop for recruiting further macrophage carriers but also unwanted cells such as Tregs and MDSCs, promoting tumor progression (Figure 6C). Moreover, CCL2 has been shown to promote macrophage polarization into the M2 phenotype and an immunosuppressive TME.[33] Importantly, our results showed that 3- and 6-day co-cultures of spheroids with M1 macrophages loaded with B_4C nanoparticles resulted in lower CCL2 levels compared to co-cultures with control M1 macrophages and other macrophage populations. Further analysis of the macrophage phenotype after co-culture with spheroids revealed that M1 macrophages did not increase CD206 expression (Figure 7). On the other hand, M2 macrophages with B_4C nanoparticles showed a decrease in CD206 expression after co-culture compared to control M2 macrophages. Moreover, increased expression of markers characteristic of the M1 phenotype (MHC II, CD40, and CD86) was observed in all BMDM populations after co-culture. This may indicate the activation of macrophages toward immunostimulation and the potential

ability to present antigens and activate T lymphocytes. These observations are supported by studies showing that spheroids obtained from certain cell lines, such as MCF-7, can polarize macrophages more strongly toward the M1 than the M2 phenotype.[34] A more common phenomenon is the repolarization of M1 macrophages toward the M2 phenotype caused by the immunosuppressive effects of the TME. However, the ability of M1 macrophages with engulfed B_4C nanoparticles to maintain this phenotype in the TME is highly desirable for supporting anticancer therapy.

Conclusion

Our studies indicate that BMDMs are promising carriers of boron carbide nanoparticles. They efficiently engulf B_4C nanoparticles and migrate across the in vitro BBB model toward the glioblastoma cell-conditioned medium. M1 macrophages appear to be the best candidates for carriers because they not only accumulate nanoparticles most efficiently but also produce less CCL2 than other populations and maintain their phenotype in the presence of cancer cells. The obtained results constitute a solid basis for further studies aimed at confirming the effectiveness of the proposed therapeutic strategy in the in vivo model and in BNCT.

Abbreviations

3D, three-dimensional; ^{4}He, helium-4 isotope - alpha particles; ^{7}Li, lithium-7 isotope; ^{10}B, boron-10 isotope; B_4C, boron carbide; BBB, blood-brain barrier; BMDMs, bone marrow-derived macrophages; BNCT, boron neutron capture therapy; CCL2, C-C motif chemokine ligand 2; CCR2, C-C chemokine receptor type 2; DLS, dynamic light scattering; DMEM, Dulbecco's modified Eagle's medium; EGF, epidermal growth factor; FBS, fetal bovine serum; FGF, fibroblast growth factor; ICP-MS, inductively coupled plasma mass spectrometry; IFN-γ, interferon-γ; IL, interleukin; LDV, laser Doppler velocimetry; LET, linear energy transfer; LPS, lipopolysaccharide; MCP-1, monocyte chemotactic protein-1; M-CSF, macrophage colony-stimulating factor; MDSCs, myeloid-derived suppressor cells; MFI, mean fluorescence intensity; MHC II, major histocompatibility complex class II; MTT, 3-(4,5-dimethylthiazol-2-yl)-2,5-diphenyltetrazolium bromide; PLGA, poly(lactide-co-glycolide); RI, refractive index; RLU, relative luminescence units; SEM, scanning electron microscope; TAMs, tumor-associated macrophages; TEER, transepithelial electrical resistance; TEM, transmission electron microscopy; TME, tumor microenvironment; TNF-α, tumor necrosis factor α; Tregs, regulatory T lymphocytes.

Data Sharing Statement

The raw data associated with the publication have been deposited in the RepOD repository [https://doi.org/10.18150/NYKOEJ].

Ethics Approval and Informed Consent

Pursuant to the Act on the Protection of Animals Used for Scientific or Educational Purposes (Journal of Laws 2015, item 266, Art. 2(6)), euthanasia of an animal solely for the purpose of using its organs or tissues is not a procedure requiring the approval of the Local Ethics Committee.

Acknowledgment

This paper has been uploaded to the bioRxiv server as a preprint [https://www.biorxiv.org/content/10.64898/2026.01.09.698353v1].

Author Contributions

All authors made a significant contribution to the work reported, whether that is in the conception, study design, execution, acquisition of data, analysis and interpretation, or in all these areas; took part in drafting, revising or critically reviewing the article; gave final approval of the version to be published; have agreed on the journal to which the article has been submitted; and agree to be accountable for all aspects of the work.

Funding

This research was funded by the National Science Center, Poland (Grant No. 2022/45/N/NZ5/03204).

Disclosure

The authors declare that they have no known competing financial interests or personal relationships that could have appeared to influence the work reported in this paper.

References

1. Liu Y, Zhou F, Ali H, Lathia JD, Chen P. Immunotherapy for glioblastoma: current state, challenges, and future perspectives. *Cell Mol Immunol*. 2024;21(12):1354–1375. doi:10.1038/s41423-024-01226-x
2. Alcantara Llaguno SR, Parada LF. Cell of origin of glioma: biological and clinical implications. *Br J Cancer*. 2016;115(12):1445–1450. doi:10.1038/bjc.2016.354
3. Miller KD, Ostrom QT, Kruchko C, et al. Brain and other central nervous system tumor statistics, 2021. *CA Cancer J Clin*. 2021;71(5):381–406. doi:10.3322/caac.21693
4. DeCordova S, Shastri A, Tsolaki AG, et al. Molecular heterogeneity and immunosuppressive microenvironment in glioblastoma. *Front Immunol*. 2020;11:1402. doi:10.3389/fimmu.2020.01402
5. Jin WH, Seldon C, Butkus M, Sauerwein W, Giap HB. A review of boron neutron capture therapy: its history and current challenges. *Int J Part Ther*. 2022;9(1):71–82. doi:10.14338/IJPT-22-00002.1
6. Coghi P, Li J, Hosmane NS, Zhu Y. Next generation of boron neutron capture therapy (BNCT) agents for cancer treatment. *Med Res Rev*. 2023;43(5):1809–1830. doi:10.1002/med.219643
7. Takeno S, Yoshino Y, Aihara T, et al. Preliminary outcomes of boron neutron capture therapy for head and neck cancers as a treatment covered by public health insurance system in Japan: real-world experiences over a 2-year period. *Cancer Med*. 2024;13(11):e7250. doi:10.1002/cam4.7250
8. Monti Hughes A, Hu N. Optimizing boron neutron capture therapy (BNCT) to treat cancer: an updated review on the latest developments on boron compounds and strategies. *Cancers*. 2023;15(16):4091. doi:10.3390/cancers15164091
9. Kozień D, Szermer-Olearnik B, Rapak A, et al. Boron-rich boron carbide nanoparticles as a carrier in boron neutron capture therapy: their influence on tumor and immune phagocytic cells. *Materials*. 2021;14(11):3010. doi:10.3390/ma14113010
10. Rudawska A, Szermer-Olearnik B, Szczygieł A, et al. Functionalized boron carbide nanoparticles as active boron delivery agents dedicated to boron neutron capture therapy. *Int J Nanomed*. 2025;20:6637–6657. doi:10.2147/IJN.S516534
11. Wang H-F, Liu Y, Yang G, Zhao C-X. Macrophage-mediated cancer drug delivery. *Mater Today Sustain*. 2021;11:100055. doi:10.1016/j.mtsust.2020.100055
12. Asimakidou E, Tan JKS, Zeng J, Lo CH. Blood-brain barrier-targeting nanoparticles: biomaterial properties and biomedical applications in translational neuroscience. *Pharmaceuticals*. 2024;17(5):612. doi:10.3390/ph17050612
13. Zhao W, Zhang Z, Xie M, et al. Exploring tumor-associated macrophages in glioblastoma: from diversity to therapy. *NPJ Precis Oncol*. 2025;9(1):126. doi:10.1038/s41698-025-00920-x
14. Xu C, Xiao M, Li X, et al. Origin, activation, and targeted therapy of glioma-associated macrophages. *Front Immunol*. 2022;13:974996. doi:10.3389/fimmu.2022.974996
15. Wróblewska A, Szczygieł A, Szermer-Olearnik B, Pajtasz-Piasecka E. Macrophages as promising carriers for nanoparticle delivery in anticancer therapy. *Int J Nanomed*. 2023;18:4521–4539. doi:10.2147/IJN.S421173
16. Strizova Z, Benesova I, Bartolini R, et al. M1/M2 macrophages and their overlaps - myth or reality? *Clin Sci*. 2023;137(15):1067–1093. doi:10.1042/CS20220531
17. Najafi M, Hashemi Goradel N, Farhood B, et al. Macrophage polarity in cancer: a review. *J Cell Biochem*. 2019;120(3):2756–2765. doi:10.1002/jcb.27646
18. Sun M, Bialasek M, Rygiel T, Weller M, Krol M, Weiss T. EXTH-75. A macrophage-based drug delivery platform for glioma treatment. *Neuro Oncol*. 2023;25(Suppl 5):v241–2. doi:10.1093/neuonc/noad179.0928
19. Pang L, Qin J, Han L, et al. Exploiting macrophages as targeted carrier to guide nanoparticles into glioma. *Oncotarget*. 2016;7(24):37081–37091. doi:10.18632/oncotarget.9464
20. Pang L, Zhu Y, Qin J, Zhao W, Wang J. Primary M1 macrophages as multifunctional carrier combined with PLGA nanoparticle delivering anticancer drug for efficient glioma therapy. *Drug Deliv*. 2018;25(1):1922–1931. doi:10.1080/10717544.2018.1502839
21. Wróblewska A, Szermer-Olearnik B, Szczygieł A, et al. Macrophages as carriers of boron carbide nanoparticles dedicated to boron neutron capture therapy. *J Nanobiotechnology*. 2024;22(1):183. doi:10.1186/s12951-024-02397-5
22. Kozień D, Żeliszewska P, Szermer-Olearnik B, et al. Synthesis and characterization of boron carbide nanoparticles as potential boron-rich therapeutic carriers. *Materials*. 2023;16(19):6534. doi:10.3390/ma16196534
23. International Organization for Standardization. Water quality - Application of inductively coupled plasma mass spectrometry (ICP-MS) - Part 2: determination of selected elements including uranium isotopes (ISO standard no. 17294-2:2023). 2023.
24. International Organization for Standardization. General requirements for the competence of reference material producers (ISO standard no. 17034:2016). 2016.
25. Brancewicz J, Wójcik N, Sarnowska Z, Robak J, Król M. The multifaceted role of macrophages in biology and diseases. *Int J Mol Sci*. 2025;26(5):2107. doi:10.3390/ijms26052107
26. Qie Y, Yuan H, von Roemeling CA, et al. Surface modification of nanoparticles enables selective evasion of phagocytic clearance by distinct macrophage phenotypes. *Sci Rep*. 2016;6(1):26269. doi:10.1038/srep26269
27. Müller J, von Bernstorff W, Heidecke CD, Schulze T. Differential S1P receptor profiles on M1- and M2-polarized macrophages affect macrophage cytokine production and migration. *Biomed Res Int*. 2017;2017:7584621. doi:10.1155/2017/7584621
28. Li R, Serrano JC, Xing H, et al. Interstitial flow promotes macrophage polarization toward an M2 phenotype. *Mol Biol Cell*. 2018;29(16):1927–1940. doi:10.1091/mbc.E18-03-0164
29. Cui K, Ardell CL, Podolnikova NP, Yakubenko VP. Distinct migratory properties of M1, M2, and resident macrophages are regulated by $\alpha_D\beta_2$ and $\alpha_M\beta_2$ integrin-mediated adhesion. *Front Immunol*. 2018;9:2650. doi:10.3389/fimmu.2018.02650

30. Gao WJ, Liu JX, Liu MN, et al. Macrophage 3D migration: a potential therapeutic target for inflammation and deleterious progression in diseases. *Pharmacol Res*. 2021;167:105563. doi:10.1016/j.phrs.2021.105563
31. Aday S, Li W, Karp JM, Joshi N. An in vitro blood-brain barrier model to study the penetration of nanoparticles. *Biol Protoc*. 2022;12(4):e4334. doi:10.21769/BioProtoc.4334
32. Francois A, Dirheimer L, Chateau A, Lassalle HP, Yakavets I, Bezdetnaya L. A macrophages-enriched head and neck tumor spheroid model to study foslip® behavior in tumor microenvironment. *Int J Nanomed*. 2023;18:6545–6562. doi:10.2147/IJN.S427350
33. Chang AL, Miska J, Wainwright DA, et al. CCL2 produced by the glioma microenvironment is essential for the recruitment of regulatory T cells and myeloid-derived suppressor cells. *Cancer Res*. 2016;76(19):5671–5682. doi:10.1158/0008-5472.CAN-16-0144
34. Madsen NH, Nielsen BS, Nhat SL, Skov S, Gad M, Larsen J. Monocyte infiltration and differentiation in 3D multicellular spheroid cancer models. *Pathogens*. 2021;10(8):969. doi:10.3390/pathogens10080969